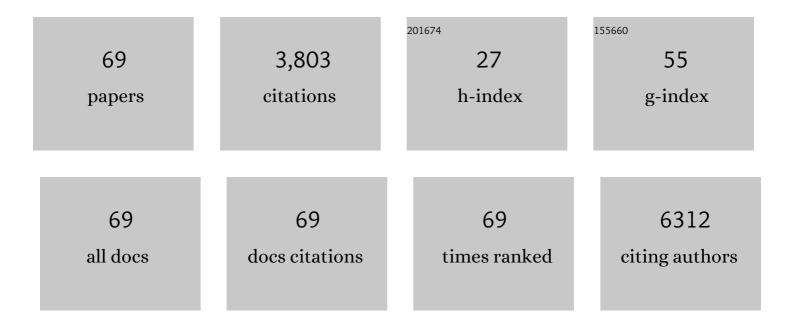
List of Publications by Year in descending order

Source: https://exaly.com/author-pdf/3724906/publications.pdf Version: 2024-02-01



WENDEL CAO

#	Article	IF	CITATIONS
1	Polarization fluctuation of BaTiO3 at unit cell level mapped by four-dimensional scanning transmission electron microscopy. Journal of Vacuum Science and Technology A: Vacuum, Surfaces and Films, 2022, 40, 013205.	2.1	4
2	Characterization of nanomaterials dynamics with transmission electron microscope. , 2022, , .		0
3	AutoDisk: Automated diffraction processing and strain mapping in 4D-STEM. Ultramicroscopy, 2022, 236, 113513.	1.9	5
4	Direct observation of elemental fluctuation and oxygen octahedral distortion-dependent charge distribution in high entropy oxides. Nature Communications, 2022, 13, 2358.	12.8	35
5	Strong electrostatic adsorption approach to the synthesis of sub-three nanometer intermetallic platinum–cobalt oxygen reduction catalysts. Nano Energy, 2021, 79, 105465.	16.0	59
6	Stretchable and Multi-Metal–Organic Framework Fabrics Via High-Yield Rapid Sorption-Vapor Synthesis and Their Application in Chemical Warfare Agent Hydrolysis. ACS Applied Materials & Interfaces, 2021, 13, 31279-31284.	8.0	13
7	Atomistic insights into the nucleation and growth of platinum on palladium nanocrystals. Nature Communications, 2021, 12, 3215.	12.8	18
8	In Situ Observations of the Dynamics of Pd@Pt Core-Shell Nanoparticles in Electrolyte. Microscopy and Microanalysis, 2021, 27, 234-236.	0.4	2
9	Phase transition and atomic scale dynamics in chemical reactions revealed in the solid state by electron microscopy. Microscopy and Microanalysis, 2021, 27, 2210-2211.	0.4	1
10	Sub-10-nm graphene nanoribbons with atomically smooth edges from squashed carbon nanotubes. Nature Electronics, 2021, 4, 653-663.	26.0	61
11	Fast Proton Insertion in Layered H ₂ W ₂ O ₇ via Selective Etching of an Aurivillius Phase. Advanced Energy Materials, 2021, 11, .	19.5	16
12	Thickness and defocus dependence of inter-atomic electric fields measured by scanning diffraction. Ultramicroscopy, 2020, 208, 112850.	1.9	14
13	Tailoring a Three-Phase Microenvironment for High-Performance Oxygen Reduction Reaction in Proton Exchange Membrane Fuel Cells. Matter, 2020, 3, 1774-1790.	10.0	71
14	From ion to atom to dendrite: Formation and nanomechanical behavior of electrodeposited lithium. MRS Bulletin, 2020, 45, 891-904.	3.5	9
15	2D metal–organic framework for stable perovskite solar cells with minimized lead leakage. Nature Nanotechnology, 2020, 15, 934-940.	31.5	258
16	Crystallinity after decarboxylation of a metal–carboxylate framework: indestructible porosity for catalysis. Dalton Transactions, 2020, 49, 11902-11910.	3.3	10
17	Multiscale Electric Field Imaging of Vortices in PbTiO3-SrTiO3 Superlattice. Microscopy and Microanalysis, 2020, 26, 466-468.	0.4	1
18	Polarization in Ferroelectric BiFeO3 Imaged in 3D Using Four-dimensional Scanning Transmission Electron Microscopy. Microscopy and Microanalysis, 2020, 26, 1132-1134.	0.4	0

#	Article	IF	CITATIONS
19	Strain-Induced Corrosion Kinetics at Nanoscale Are Revealed in Liquid: Enabling Control of Corrosion Dynamics of Electrocatalysis. CheM, 2020, 6, 2257-2271.	11.7	48
20	Transmission Electron Microscopy of Catalytic Nanomaterials at Atomic Resolution. Microscopy and Microanalysis, 2019, 25, 2054-2055.	0.4	0
21	Measuring Charge State at the Single-Atomic-Column-Base with Four-Dimensional Scanning Transmission Electron Microscopy. Microscopy and Microanalysis, 2019, 25, 16-17.	0.4	0
22	Strong Electronic Interaction of Amorphous Fe ₂ O ₃ Nanosheets with Singleâ€Atom Pt toward Enhanced Carbon Monoxide Oxidation. Advanced Functional Materials, 2019, 29, 1904278.	14.9	51
23	Structures and electronic properties of domain walls in BiFeO3 thin films. National Science Review, 2019, 6, 669-683.	9.5	18
24	Differential Surface Elemental Distribution Leads to Significantly Enhanced Stability of PtNi-Based ORR Catalysts. Matter, 2019, 1, 1567-1580.	10.0	82
25	<i>In situ</i> Cathodoluminescence and Monitoring Electronic Structure Change Using Optical TEM Holder. Microscopy and Microanalysis, 2019, 25, 2302-2303.	0.4	1
26	In Situ Observations of Abnormal Pore Size Changes of a Zirconium Based Metal-Organic Framework Using Atomic Resolution S/TEM and EELS. Microscopy and Microanalysis, 2019, 25, 1486-1487.	0.4	1
27	Charge Density Mapping via Scanning Diffraction in Scanning Transmission Electron Microscopy. Microscopy and Microanalysis, 2019, 25, 18-19.	0.4	0
28	Probing the dynamics of nanoparticle formation from a precursor at atomic resolution. Science Advances, 2019, 5, eaau9590.	10.3	40
29	Freestanding crystalline oxide perovskites down to the monolayer limit. Nature, 2019, 570, 87-90.	27.8	398
30	Tunable intrinsic strain in two-dimensional transition metal electrocatalysts. Science, 2019, 363, 870-874.	12.6	384
31	Real-space charge-density imaging with sub-ångström resolution by four-dimensional electron microscopy. Nature, 2019, 575, 480-484.	27.8	127
32	Nanoscale kinetics of asymmetrical corrosion in core-shell nanoparticles. Nature Communications, 2018, 9, 1011.	12.8	87
33	Self-assembling epitaxial growth of a single crystalline CoFe ₂ O ₄ nanopillar array <i>via</i> dual-target pulsed laser deposition. Journal of Materials Chemistry C, 2018, 6, 4854-4860.	5.5	4
34	Intercorrelated In-Plane and Out-of-Plane Ferroelectricity in Ultrathin Two-Dimensional Layered Semiconductor In ₂ Se ₃ . Nano Letters, 2018, 18, 1253-1258.	9.1	509
35	Tuning Fe concentration in epitaxial gallium ferrite thin films for room temperature multiferroic properties. Acta Materialia, 2018, 145, 488-495.	7.9	26
36	Engineering Temperatureâ€Dependent Carrier Concentration in Bulk Composite Materials via Temperatureâ€Dependent Fermi Level Offset. Advanced Energy Materials, 2018, 8, 1701623.	19.5	21

#	Article	IF	CITATIONS
37	Core–Shell Nanostructured Cobalt–Platinum Electrocatalysts with Enhanced Durability. ACS Catalysis, 2018, 8, 35-42.	11.2	72
38	Combined In Situ and Ex Situ Study on Synthesis of Nanostructured Catalyst in Solid State. Microscopy and Microanalysis, 2018, 24, 288-289.	0.4	0
39	Direct in Situ Observation and Analysis of the Formation of Palladium Nanocrystals with High-Index Facets. Nano Letters, 2018, 18, 7004-7013.	9.1	42
40	Large Negative-Thermal-Quenching Effect in Phonon-Induced Light Emissions in Mn ⁴⁺ -Activated Fluoride Phosphor for Warm-White Light-Emitting Diodes. ACS Omega, 2018, 3, 13704-13710.	3.5	41
41	In situ Atmospheric Transmission Electron Microscopy of Catalytic Nanomaterials. MRS Advances, 2018, 3, 2297-2303.	0.9	2
42	Neighboring Pt Atom Sites in an Ultrathin FePt Nanosheet for the Efficient and Highly CO-Tolerant Oxygen Reduction Reaction. Nano Letters, 2018, 18, 5905-5912.	9.1	84
43	Surface-Engineered PtNi-O Nanostructure with Record-High Performance for Electrocatalytic Hydrogen Evolution Reaction. Journal of the American Chemical Society, 2018, 140, 9046-9050.	13.7	379
44	Deterministic, Reversible, and Nonvolatile Low-Voltage Writing of Magnetic Domains in Epitaxial BaTiO ₃ /Fe ₃ O ₄ Heterostructure. ACS Nano, 2018, 12, 9558-9567.	14.6	43
45	Interfaces in Heterogeneous Catalysts: Advancing Mechanistic Understanding through Atomic-Scale Measurements. Accounts of Chemical Research, 2017, 50, 787-795.	15.6	128
46	Dissolution Kinetics of Oxidative Etching of Cubic and Icosahedral Platinum Nanoparticles Revealed by <i>in Situ</i> Liquid Transmission Electron Microscopy. ACS Nano, 2017, 11, 1696-1703.	14.6	84
47	Boosting phonon-induced luminescence in red fluoride phosphors <i>via</i> composition-driven structural transformations. Journal of Materials Chemistry C, 2017, 5, 12105-12111.	5.5	11
48	In situ Study of Dynamics of CuAu Alloy Nanoparticles on Oxide Supports. Microscopy and Microanalysis, 2017, 23, 954-955.	0.4	0
49	Platinumâ€Based Nanowires as Active Catalysts toward Oxygen Reduction Reaction: In Situ Observation of Surfaceâ€Diffusionâ€Assisted, Solidâ€State Oriented Attachment. Advanced Materials, 2017, 29, 1703460.	21.0	102
50	Dynamics of Transformation from Platinum Icosahedral Nanoparticles to Larger FCC Crystal at Millisecond Time Resolution. Scientific Reports, 2017, 7, 17243.	3.3	9
51	Transmission electron microscopy with atomic resolution under atmospheric pressures. MRS Communications, 2017, 7, 798-812.	1.8	24
52	Revealing Surface Elemental Composition and Dynamic Processes Involved in Facet-Dependent Oxidation of Pt ₃ Co Nanoparticles via <i>in Situ</i> Transmission Electron Microscopy. Nano Letters, 2017, 17, 4683-4688.	9.1	71
53	Calculation of the Electric Field Based on Average Momentum Transfer Using Pixelated Electron Detector in STEM. Microscopy and Microanalysis, 2017, 23, 2104-2105.	0.4	0
54	In Situ Observation of Pt Icosahedral Nanoparticles Transformation into FCC Single Crystal. Microscopy and Microanalysis, 2016, 22, 766-767.	0.4	0

#	Article	IF	CITATIONS
55	Evolution of Au 25 (SR)18 Nanoclusters on Ceria Surfaces during in situ Electron Beam Irradiation. Microscopy and Microanalysis, 2016, 22, 1278-1279.	0.4	0
56	Materials Processes Observed using Dynamical Environmental TEM at University of Illinois. Microscopy and Microanalysis, 2015, 21, 2323-2324.	0.4	0
57	Direct Observation of Interfacial Au atoms Using STEM Depth Sectioning. Microscopy and Microanalysis, 2015, 21, 2417-2418.	0.4	0
58	An Ionâ€Exchange Promoted Phase Transition in a Liâ€Excess Layered Cathode Material for Highâ€Performance Lithium Ion Batteries. Advanced Energy Materials, 2015, 5, 1401937.	19.5	82
59	Growth of Au on Pt Icosahedral Nanoparticles Revealed by Low-Dose In Situ TEM. Nano Letters, 2015, 15, 2711-2715.	9.1	106
60	Direct Observation of Interfacial Au Atoms on TiO ₂ in Three Dimensions. Nano Letters, 2015, 15, 2548-2554.	9.1	26
61	Atomic resolution tomography reconstruction of tilt series based on a GPU accelerated hybrid input–output algorithm using polar Fourier transform. Ultramicroscopy, 2015, 149, 64-73.	1.9	6
62	Oxidation of Fe Whiskers and Surface Diffusion Observed by Environmental TEM. Microscopy and Microanalysis, 2014, 20, 1864-1865.	0.4	1
63	Lattice and strain analysis of atomic resolution Z-contrast images based on template matching. Ultramicroscopy, 2014, 136, 50-60.	1.9	80
64	A kinetic Monte Carlo study of coarsening resistance of novel core/shell precipitates. Acta Materialia, 2014, 79, 37-46.	7.9	4
65	Interaction of nanometer-sized gold nanocrystals with rutile (110) surface steps revealed at atomic resolution. Surface Science, 2014, 625, 16-22.	1.9	15
66	Measurement of Local Atomic Displacements Reveals Interaction of Au Nanocrystals with Rutile (TiO2) Surface Steps. Microscopy and Microanalysis, 2014, 20, 1072-1073.	0.4	0
67	Imaging Shape-Dependent Corrosion Behavior of Pt Nanoparticles over Extended Time Using a Liquid Flow Cell and TEM. Microscopy and Microanalysis, 2014, 20, 1508-1509.	0.4	9
68	Surface Atomic Diffusion Processes Observed at Milliseconds Time Resolution using Environmental TEM. Microscopy and Microanalysis, 2014, 20, 1590-1591.	0.4	0
69	In situ RHEED study of epitaxial gold nanocrystals on TiO2 (110) surfaces. Applied Surface Science, 2013, 270, 661-666.	6.1	8